

# INTERNATIONAL SOCIETY FOR SOIL MECHANICS AND GEOTECHNICAL ENGINEERING



*This paper was downloaded from the Online Library of the International Society for Soil Mechanics and Geotechnical Engineering (ISSMGE). The library is available here:*

<https://www.issmge.org/publications/online-library>

*This is an open-access database that archives thousands of papers published under the Auspices of the ISSMGE and maintained by the Innovation and Development Committee of ISSMGE.*

# Modelling of constitutive behavior of sand in the low stress regime: an implementation of SANISAND

Modélisation du comportement constitutif du sable dans un régime à faible contrainte: mise en œuvre sur SANISAND

Chiara Latini, Varvara Zania

*Civil Engineering Department, Technical University of Denmark, Denmark, chila@byg.dtu.dk*

Claudio Tamagnini

*Civil Engineering Department, University of Perugia, Italy*

**ABSTRACT:** The paper provides background information for the modification of SANISAND (2004) constitutive model in order to capture the mechanical behavior of sand in the low stress regime. In the implementation of this model in finite element programs, computational difficulties arise due to the gradient discontinuity which occurs at the apex of the yield surface when it deals with soil deposits subjected to low initial confining pressure. This singularity often causes the stress-point integration algorithm to perform inefficiently or even fail. In this study a hyperbolic yield surface was introduced to eliminate the singular tip from the original yield surface, by adjusting only one parameter. Undrained triaxial compression tests on Toyoura sand are performed to show the performance of the proposed formulation.

**RÉSUMÉ:** Cet article fournit des informations de base pour la modification du modèle constitutif de SANISAND (2004) afin de cerner le comportement mécanique du sable dans un régime à faible contrainte. Lors de l'utilisation de ce modèle dans des logiciels à éléments finis, des problèmes de calcul apparaissent à cause de la discontinuité du gradient qui se produit au sommet de la surface de limite élastique, pour des dépôts de sol soumis à une faible pression initiale de confinement. Cette singularité provoque souvent une mauvaise exécution de l'algorithme d'intégration des points de contrainte, voir son échec. Dans cette étude, une surface de limite élastique hyperbolique a été introduite pour éliminer le point singulier de la surface de limite élastique initiale, en ajustant uniquement un paramètre. Des essais de compression triaxiale non drainés sur du sable de Toyoura sont effectués pour montrer la performance de la formulation proposée.

**KEYWORDS:** anisotropy; sand; constitutive relations; plasticity; critical state, hyperbolic approximation

## 1 INTRODUCTION

Understanding the behavior of offshore marine sands subjected to cyclic loadings is essential for predicting the response of offshore foundations under monotonic and cyclic loading conditions. Therefore, it is necessary a constitutive material model that properly describes the characteristic behavior of water saturated soil under cyclic loading.

Constitutive models based on perfect plasticity are capable to reproduce nonlinearity and irreversible behavior of the soil when it is subjected to monotonic loadings. On the contrary, they are not sufficient to describe the highly non-linear stress path dependent shear stiffness, the accumulation of pore pressure, permanent shear strains and volumetric strains under repeated number of cycles. In the last two decades several advanced constitutive models (Cubrinovski and Ishihara 1998, Gajo and Wood 1999, Mroz and Pietruszczak 1983, Wang et al. 1990) have been carried out to investigate the cyclic/dynamic behavior of sands.

The three dimensional critical state two-surface plasticity models for sands proposed by Dafalias and Manzari (2004) is a conceptually simple constitutive model, which adequately describes induced anisotropy, history-dependent dilatancy and fabric evolution of sands. It is part of the SANISAND (Simple ANIso-tropic SAND) models developed by Dafalias and collaborators (Manzari and Dafalias 1997, Li and Dafalias 2000, Dafalias and Manzari 2004, Dafalias et al. 2004, Taiebat and Dafalias 2007).

Furthermore, this version of SANISAND has been implemented as a User defined Material (UMAT) code in Fortran

for the Finite Element Code ABAQUS (Gudehus et al. 2008) and it can also be compiled together with IncrementalDriver (Niemunis 2008). Nonetheless, the implementation of SANISAND (2004) model in finite element programs involves computational difficulties due to the gradient discontinuities which occur at the tip of the yield surface. This implies that inefficient performance of the stress integration scheme might be experienced when the response of soil deposits in the low stress regime is investigated.

The objective of the present study is to propose a formulation which is able to model the mechanical behavior of sand subjected to low initial confining pressure. Therefore, the formulation aims at introducing a rounded hyperbolic yield surface to eliminate the singular apex from the original yield criterion. Due to this modification, the model is denoted the modified SANISAND (2004) model. The modification of the constitutive model is shown in details in multiaxial formulation. In addition, the performance of the modified SANISAND (2004) model is presented with respect to that of the original model (Dafalias and Manzari, 2004) to simulate undrained triaxial compression tests for loose sand subjected to low initial confining pressure.

### 1.1 Notation and assumptions

In this study the soil mechanics convention is considered, where compression is assumed positive and effective stresses are taken into account.

To represent vector and tensor quantities, the following standard notation is adopted. For any two vectors,  $\mathbf{u}, \mathbf{v} \in \mathbb{R}^3$ , the dot product is defined as:  $\mathbf{u} \cdot \mathbf{v} = u_i v_i$  and the dyadic product as

$[\mathbf{v} \otimes \mathbf{w}]_{ij} = v_i w_j$ . For any two second-order tensors  $\mathbf{X}, \mathbf{Y} \in \mathcal{L}$ ,  $\mathbf{X} \cdot \mathbf{Y} = X_{ij} Y_{ij}$  and  $[\mathbf{X} \otimes \mathbf{Y}]_{ijkl} = X_{ij} Y_{kl}$ . The quantity  $\|\mathbf{X}\| = \sqrt{\mathbf{X} \cdot \mathbf{X}}$  represents the Euclidean norm of the second-order tensor  $\mathbf{X}$ .

Considering small deformations and rotations, the total strain rate can be divided into elastic ( $\dot{\boldsymbol{\epsilon}}^e$ ) and plastic term ( $\dot{\boldsymbol{\epsilon}}^p$ ):

$$\dot{\boldsymbol{\epsilon}} = \dot{\boldsymbol{\epsilon}}^e + \dot{\boldsymbol{\epsilon}}^p \quad (1)$$

where  $\boldsymbol{\epsilon}$  is the strain tensor.

## 2 THE MODIFIED SANISAND (2004) MODEL IN TRIAXIAL SPACE

### 2.1 Yield surface

In the proposed formulation the elastic stress-strain relationship is defined as reported in the work of Dafalias and Manzari (2004). Regarding the yield surface, SANISAND (2004) constitutive model suggested the following expression:

$$f = \{(\mathbf{s} - p\boldsymbol{\alpha}) \cdot (\mathbf{s} - p\boldsymbol{\alpha})\}^{1/2} - \sqrt{\frac{2}{3}} mp = 0 \quad (2)$$

where  $\mathbf{s}$  is the deviatoric stress tensor and  $p$  is the pressure. While the stress-ratio quantity  $\boldsymbol{\alpha}$  is called the back-stress ratio and it is the rotational hardening variable of the yield surface, which represents the slope in  $p$ - $q$  space of the bisector of the yield surface. The coefficient  $m$  is the tangent of half the opening angle of the yield surface at the origin. However, the open conical yield surface is characterized by a singular point, which is the apex as shown in Figure 1.

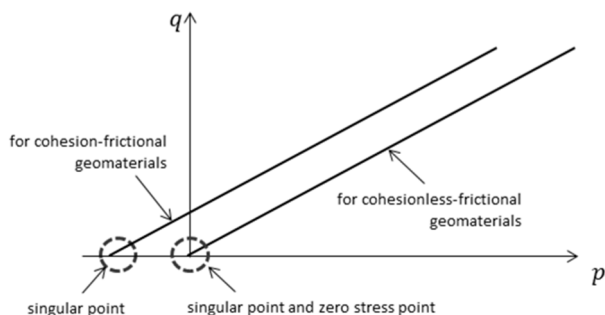


Figure 1: SANISAND (2004) yield surface in  $p$ - $q$  plane.

In order to avoid the gradient discontinuity at the apex, a hyperbolic yield surface was introduced. Therefore, the yield surface was regularized by adopting the trigonometric rounding technique of Sloan and Booker (1986). The main features of this yield surface are: 1) continuous and differentiable at all stress states and 2) approximate SANISAND (2004) yield function as closely as required by adjusting one parameter. The model still maintains an open conical yield surface, which can rotate around the cone apex at the origin of the stress space, and three additional open wedge-type surfaces with apex at the origin of stress space: the critical state surface (CSS), the bounding surface (BS) and the dilatancy surface (DS).

In the present formulation the cohesion  $c$  was first introduced as  $p_t = c \cot \phi$  and then, the hydrostatic pressure  $p^*$  is given as:

$$p^* = p + p_t \quad (3)$$

where  $\phi$  is the friction angle. The distance between the vertex of the original yield surface and the hyperbolic yield surface is defined by the constant parameter  $b$ , which is a fraction of  $p_t$ :

$$b = \eta p_t, \text{ with } \eta \in (0,1) \quad (4)$$

Therefore, the hyperbolic yield function can be written as follows:

$$f = \{(\mathbf{s} - p^*\boldsymbol{\alpha}) \cdot (\mathbf{s} - p^*\boldsymbol{\alpha}) + (mb)^2\}^{1/2} - \sqrt{\frac{2}{3}} mp = 0 \quad (5)$$

In the triaxial stress plane the equation of the yield surface is proposed in terms of the triaxial stress quantities  $p = (\sigma_1 + 2\sigma_3)/3$  and  $q = (\sigma_1 - \sigma_3)$ , where  $\sigma_1$  and  $\sigma_3$  are respectively the maximum and the minimum principle stress:

$$f^* = \{(q - \alpha p^*)^2 + m^2 b^{*2}\}^{1/2} - mp^* = 0 \quad (6)$$

where  $b^* = \sqrt{3/2}b$ .

In Figure 2a and 2b the yield surface of the modified SANISAND (2004) model is illustrated in triaxial stress plane and in the multiaxial space, respectively along with the CSS ( $\alpha^c$ ), the BS ( $\alpha^b$ ) and the DS ( $\alpha^d$ ).

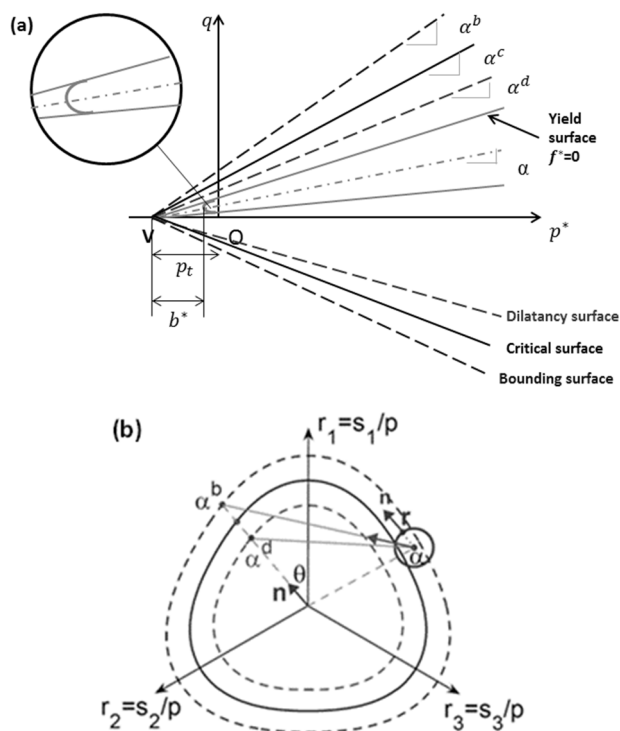


Figure 2: The yield surface of the modified SANISAND (2004) model in  $q$ - $p^*$  plane (a) and in the multiaxial space (b).

Several meridional sections of the hyperbolic yield surface are plotted in Figure 3a, varying the parameter  $b^*$  and setting the hardening variable  $\alpha$  equal to zero. Recall that the hyperbolic yield surface closely represents the original yield surface for  $b^* \leq 0.25p_t$ . While the effect of the back stress ratio is investigated by considering  $b^* = p_t$ , see Figure 3b.

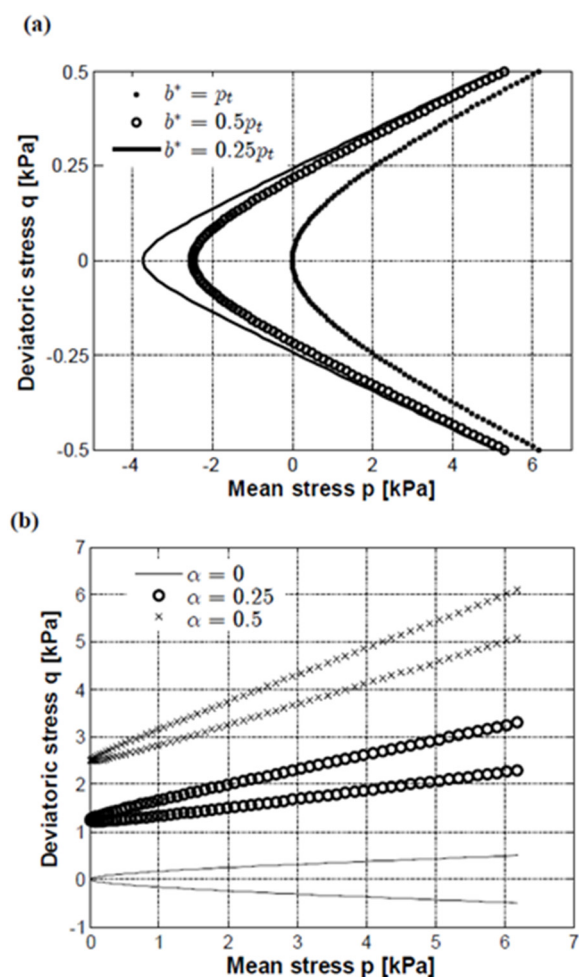


Figure 3: Effect of  $b^*$  parameter (a) and the back stress ratio  $\alpha$  (b) on the hyperbolic yield surface in  $q$ - $p$  plane.

The formulation of the critical state, bounding and dilatancy surfaces are considered depending on the back stress ratio  $\alpha$  and they are defined as in the work of Dafalias and Manzari (2004). Note that in the original formulation the dependency of CSS, BS and DS in the  $q$ - $p$  space on the Lode angle  $\theta$  is given by the expression suggested by Argyris et al. (1974). Nevertheless, the implementation of the modified SANISAND (2004) takes into account the expression suggested by Van Eekelen (Van Eekelen, 1980), which is more accurate for high values of the critical state friction angle (Lin and Bazant, 1986).

## 2.2 Flow rule

The plastic flow direction is defined as:

$$\dot{\epsilon}^p = \dot{\gamma} \mathbf{R} \quad (7)$$

Where  $\dot{\gamma} \geq 0$  and it represents the plastic multiplier.  $\mathbf{R}$  is the plastic potential, which is expressed as follows:

$$\mathbf{R} = \frac{\partial g}{\partial \boldsymbol{\sigma}} = \mathbf{n} + \frac{1}{3} D \mathbf{1} \quad (8)$$

Where  $\mathbf{n} = (\mathbf{s} - p^* \boldsymbol{\alpha}) / \|\mathbf{s} - p^* \boldsymbol{\alpha}\|$  and  $D$  is the dilatancy coefficient. The flow rule is still considered non-associative as in SANISAND (2004) model and  $D$  is given as:

$$D = x D_{DM} = \begin{cases} D = D_{DM}, & x = 1, \text{ if } p > p_t \\ D = x D_{DM}, & \text{if } p \in [0; p_t] \\ D = 0, & \text{if } p < 0 \end{cases} \quad (9)$$

Where  $x = \frac{p}{p_t}$  and  $D_{DM}$  is the dilatancy coefficient defined by Dafalias and Manzari (2004). This implies that  $D$  depends on the variation of the plastic volumetric strain, which was assumed zero for negative values of the mean pressure. The linear interpolation of the dilatancy coefficient in the interval  $[0, p_t]$  was taken into account in order to have zero change in volume at the critical state and have a plastic potential function which varies in the proximity of the apex of the hyperbole. In addition, these assumptions may be considered valid, since the area subjected to regularization is small  $[-p_t, p_t]$ .

The loading index  $L$  is obtained by applying the consistency condition  $\dot{f}^* = 0$  and yields to:

$$L = \frac{1}{K_p} \left( \frac{\partial f^*}{\partial p^*} \frac{\partial p^*}{\partial \boldsymbol{\sigma}} + \frac{\partial f^*}{\partial \mathbf{s}} \frac{\partial \mathbf{s}}{\partial \boldsymbol{\sigma}} \right) \quad (10)$$

$$K_p = - \left( \frac{\partial f^*}{\partial \boldsymbol{\alpha}} \boldsymbol{\alpha} \right) \quad (11)$$

The partial derivatives of the yield surface with respect to the stress and the internal variables can be determined as follows:

$$\begin{aligned} \frac{\partial f^*}{\partial \boldsymbol{\sigma}} &= \frac{\partial f^*}{\partial p^*} \frac{\partial p^*}{\partial \boldsymbol{\sigma}} + \frac{\partial f^*}{\partial \mathbf{s}} \frac{\partial \mathbf{s}}{\partial \boldsymbol{\sigma}} = \\ &= \frac{1}{A_1} \left\{ (\mathbf{s} - p^* \boldsymbol{\alpha}) - \frac{1}{3} \mathbf{1} [\boldsymbol{\alpha} \cdot (\mathbf{s} - p^* \boldsymbol{\alpha})] \right\} - \frac{1}{3} \sqrt{\frac{2}{3}} m^2 \mathbf{1} \end{aligned} \quad (12)$$

$$\frac{\partial f^*}{\partial \boldsymbol{\alpha}} = - \frac{1}{A_1} p^* (\mathbf{s} - p^* \boldsymbol{\alpha}) \quad (13)$$

Where

$$\frac{\partial f^*}{\partial \mathbf{s}} = \frac{1}{A_1} (\mathbf{s} - p^* \boldsymbol{\alpha}) \quad (14)$$

$$\frac{\partial \mathbf{s}}{\partial \boldsymbol{\sigma}} = \mathbf{1} - \frac{1}{3} \mathbf{1} \otimes \mathbf{1} \quad (15)$$

$$\frac{\partial f^*}{\partial p} = \frac{1}{A_1} (\mathbf{s} - p^* \boldsymbol{\alpha}) \cdot (-\boldsymbol{\alpha}) - \sqrt{\frac{2}{3}} m \quad (16)$$

$$\frac{\partial p}{\partial \boldsymbol{\sigma}} = \frac{1}{3} \mathbf{1} \quad (17)$$

$$\text{With } A_1 = \sqrt{(\mathbf{s} - p^* \boldsymbol{\alpha}) \cdot (\mathbf{s} - p^* \boldsymbol{\alpha}) + \frac{2}{3} m^2 b^*{}^2}.$$

## 3 THE MODIFIED SANISAND (2004) IN THE LOW STRESS REGIME

The implementation of the modified SANISAND (2004) model in finite element code was performed by modifying the subroutine freely available on the open-source database of constitutive models soilmodels.info (Gudehus et al., 2008). The modified SANISAND (2004) was implemented in the code by deploying an explicit, adaptive stress-point algorithm with error control, based on Runge-Kutta-Fehlberg scheme of third order (RKF-32) to integrate the constitutive equations at the Gauss point level.

In this section the performance of the stress integration scheme of the modified SANISAND (2004) model is compared with respect to that of the original constitutive soil model for the case of low stress regime, see Figure 4. The simulations of

undrained triaxial tests for loose sandy sample ( $e_0=0.996$ ) were carried out by deploying IncrementalDriver (Niemunis, 2008). In addition, the analyses were conducted setting  $p_t = 5\text{kPa}$  and initial hydrostatic pressure  $p_0 = 30\text{kPa}$ . Note that the material constants considered are those referred to Toyoura sand, which are listed in the work of Dafalias and Manzari (2004).

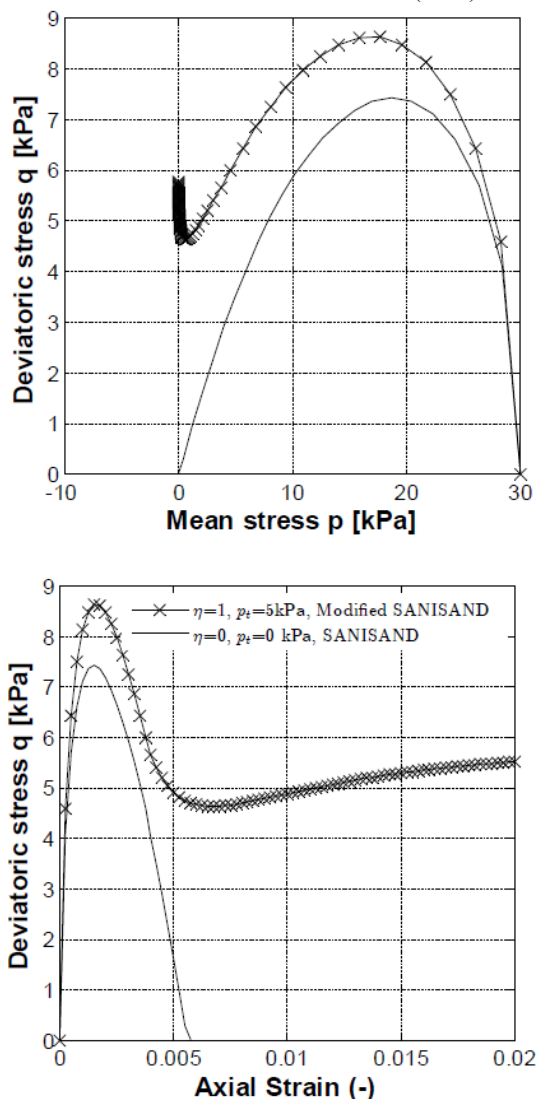


Figure 4: Monotonic undrained compression triaxial test on Toyoura sand. Comparison between the performance of SANISAND (2004) and the modified SANISAND (2004) model.

The outcomes highlighted that in the new formulation the stress integration does not fail as in the original formulation, when it deals with sandy soil deposits subjected to low initial confining pressure.

In addition, the algorithm was tested by decreasing the number of increments of the strain step applied ( $N_{incr} = 500, 100$  and  $50$ ). First, it was observed that the outcomes of the simulations overlapped the results obtained by setting  $N_{incr} = 1000$  for a given error tolerance of the explicit, adaptive stress-point algorithm ( $TOL = 10^{-5}$ ). A relative error with respect to the exact solutions of  $\sigma$  and  $\alpha$ , obtained numerically by deploying the RKF23 for error tolerance of  $TOL = 10^{-6}$ , was calculated for each simulation. Results showed that a relative error of  $ERR_{\sigma,\alpha} = 10^{-6}$  was achieved assuming  $N_{incr} = 500$ . While the accuracy of the algorithm was estimated for the following tolerance values:  $TOL = 10^{-5}, 10^{-4}$  and  $10^{-3}$ . It was noticed that the accuracy of the

solution decreased by increasing the tolerance constant TOL. Furthermore, it was possible to obtain a relative error  $ERR_{\sigma,\alpha} \leq 10^{-4}$ , by setting the error tolerance not larger than  $10^{-4}$ .

#### 4 CONCLUSION

A smooth hyperbolic approximation to SANISAND (2004) yield function is derived. The rounded hyperbolic surface is continuous and differentiable for all stress states, and it can approximate the original yield surface by adjusting one parameter. The present modification does not alter the features of the previous version of SANISAND (2004).

#### 5 ACKNOWLEDGEMENTS

This work has been supported by the Danish Council for Strategic Research through the project “Advancing BeYondShallow waterS (ABYSS) - Optimal design of offshore wind turbine support structures”.

#### 6 REFERENCES

Argyris J.H., Faust G., Szimmat J., Warnke P. and William K. 1974. Recent developments in finite elements analyses of prestressed concrete reactor vessels. *Nuclear Engineering and Design* 28, 42–75.

Cubrinovski M. and Ishihara K. 1998. State concept and modified elastoplasticity for sand modelling. *Soils Foundation* 38(4):213–225

Dafalias Y.F. and Manzari M.T. 2004. Simple plasticity sand model accounting for fabric change effects. *Journal of Engineering Mechanics* 130(6):622–634.

Dafalias Y.F., Papadimitriou A.G. and Li X.S. 2004. Sand plasticity model accounting for inherent fabric anisotropy. *Journal of Engineering Mechanics* 130(1): 1319-1333.

Gajo A. and Wood D.M. 1999. A kinematic hardening constitutive model for sands: the multi-axial formulation. *International Journal for Numerical and Analytical Methods in Geomechanics* 23:925-965

Gudehus G., Amorosi A., Gens A., Herle I., Kolymbas D., Masín D., Muir Wood D., Niemunis A., Nova R., Pastor M. et al. 2008. The soilmodels.info project. *International Journal for Numerical and Analytical Methods in Geomechanics* 32(12):1571–1572. <http://www.soilmodels.info>

Li X.S. and Dafalias Y.F. 2000. Dilatancy for cohesionless soils. *Geotechnique* 54(4): 499-460.

Lin F.B. and Bazant Z.P. 1986 Convexity of smooth yield surface of frictional material. *Journal of Engineering Mechanics* 112 1259–62.

Manzari M.T. and Dafalias, Y.F. 1997. A critical state two-surface plasticity model for sands. *Geotechnique* 42(2): 255-272.

Mroz Z. and Pietruszczak S. 1983. A constitutive model for sand and its application to cyclic loading. *International Journal for Numerical and Analytical Methods in Geomechanics* 7:305–320

Niemunis A. 2008 IncrementalDriver users’s manual URL <http://www.rz.uni-karlsruhe.de/gn99>

Sloan S.W. and Booker J.R. 1986 Removal singularities in Tresca and Mohr-Coloumb yield functions. *Communications in Applied Numerical Methods* 2:173-179.

Taiebat M. and Dafalias Y.F. 2007. SANISAND: simple anisotropic sand plasticity model. *International Journal for Numerical and Analytical Methods in Geomechanics* 32(8): 915-948.

Van Eekelen H.A.M. 1980. Isotropic yield surfaces in three dimensions for use in soil mechanics. *International Journal for Numerical and Analytical Methods in Geomechanics* 4, 89–101.

Wang Z.L., Dafalias Y.F. and Shen C.K. 1990. Bounding surface hypoplasticity model for sand. *Journal of Engineering Mechanics* ASCE 116(5):983–1001